Journal of Visualized Experiments

Displacement analysis of myocardial mechanical deformation (DIAMOND) reveals segmental heterogeneity of cardiac function in embryonic zebrafish
--Manuscript Draft--

Article Type:	Invited Methods Article - JoVE Produced Video
Manuscript Number:	JoVE60547R1
Full Title:	Displacement analysis of myocardial mechanical deformation (DIAMOND) reveals segmental heterogeneity of cardiac function in embryonic zebrafish
Section/Category:	JoVE Bioengineering
Keywords:	Cardiac function, Displacement, Chemotherapy, Injury, Regeneration, Zebrafish
Corresponding Author:	René R. Sevag Packard UNITED STATES
Corresponding Author's Institution:	
Corresponding Author E-Mail:	rpackard@mednet.ucla.edu
Order of Authors:	Junjie Chen
	René R. Sevag Packard
Additional Information:	
Question	Response
Please indicate whether this article will be Standard Access or Open Access.	Standard Access (US$2,400)
Please indicate the **city, state/province, and country** where this article will be **filmed**. Please do not use abbreviations.	Los Angeles, California, United States

UNIVERSITY OF CALIFORNIA, LOS ANGELES

UCLA

BERKELEY • DAVIS • IRVINE • LOS ANGELES • MERCED • RIVERSIDE • SAN DIEGO • SAN FRANCISCO

SANTA BARBARA • SANTA CRUZ

René Rupen Sevag Packard, MD, PhD
Assistant Professor-in-Residence
Division of Cardiology, Department of Medicine
David Geffen School of Medicine
University of California, Los Angeles

Center for Health Sciences Room 17-054A
10833 Le Conte Avenue, Los Angeles, CA 90095-1679
Phone: 310 825 4467
Fax: 310 206 2420
Email: rpackard@mednet.ucla.edu

Los Angeles, October 14, 2019

Kyle Jewhurst, PhD
Science Editor, *Journal of Visualized Experiments (JoVE)*

Re: Displacement analysis of myocardial mechanical deformation (DIAMOND) reveals segmental heterogeneity of cardiac function in embryonic zebrafish (JoVE60547)

Dear Dr. Jewhurst, JoVE editors and reviewers,

Thank you for offering us the opportunity to re-submit the above captioned manuscript for consideration in *JoVE.* We have responded to all the points raised by the editor and reviewers in a point-by-point manner. This manuscript expands on a novel technique we recently reported [Chen J. *et al.*; *JCI Insight* 2019 Apr 18;4(8)] for the measurement of segmental cardiac mechanics in zebrafish in a high-throughput manner.

Thank you for your consideration.

Sincerely,

René R. Sevag Packard

1 **TITLE:**
2 **Displacement Analysis of Myocardial Mechanical Deformation (DIAMOND) Reveals Segmental**
3 **Heterogeneity of Cardiac Function in Embryonic Zebrafish**
4
5 **AUTHORS AND AFFILIATIONS:**
6 Junjie Chen[1], René R. Sevag Packard[2]
7
8 [1]Division of Cardiology, Department of Medicine
9 David Geffen School of Medicine at University of California, Los Angeles
10
11 [2]Division of Cardiology, Department of Medicine
12 David Geffen School of Medicine at University of California, Los Angeles
13 Ronald Reagan UCLA Medical Center, Veterans Affairs West Los Angeles Medical Center
14
15 **Corresponding Author:**
16 René R. Sevag Packard   (RPackard@mednet.ucla.edu)
17
18 **Email Address of Co-author:**
19 Junjie Chen   (junjie93@ucla.edu)
20
21 **KEYWORDS:**
22 cardiac function, displacement, chemotherapy, injury, regeneration, zebrafish
23
24 **SUMMARY:**
25 The goal of this protocol is to detail a novel method for the assessment of segmental cardiac
26 function in embryonic zebrafish under both physiological and pathological conditions.
27
28 **ABSTRACT:**
29 Zebrafish are increasingly utilized as a model organism for cardiomyopathies and regeneration.
30 Current methods evaluating cardiac function fail to reliably detect segmental mechanics and are
31 not readily feasible in zebrafish. Here we present a semiautomated, open-source method for the
32 quantitative assessment of four-dimensional (4D) segmental cardiac function: displacement
33 analysis of myocardial mechanical deformation (DIAMOND). Transgenic embryonic zebrafish
34 were imaged in vivo using a light-sheet fluorescence microscopy system with 4D cardiac motion
35 synchronization. Acquired 3D digital hearts were reconstructed at end-systole and end-diastole,
36 and the ventricle was manually segmented into binary datasets. Then, the heart was reoriented
37 and isotropically resampled along the true short axis, and the ventricle was evenly divided into
38 eight portions (I–VIII) along the short axis. Due to the different resampling planes and matrices
39 at end-systole and end-diastole, a transformation matrix was applied for image registration to
40 restore the original spatial relationship between the resampled systolic and diastolic image
41 matrices. After image registration, the displacement vector of each segment from end-systole to
42 end-diastole was calculated based on the displacement of mass centroids in three dimensions
43 (3D). DIAMOND shows that basal myocardial segments adjacent to the atrioventricular canal
44 undergo the highest mechanical deformation and are the most susceptible to doxorubicin-

45 induced cardiac injury. Overall, DIAMOND provides novel insights into segmental cardiac
46 mechanics in zebrafish embryos beyond traditional ejection fraction (EF) under both
47 physiological and pathological conditions.
48
49 **INTRODUCTION:**
50 Chemotherapy-induced cardiac toxicity and ensuing heart failure are one of the main reasons for
51 chemotherapy discontinuation[1]. Therefore, cardiac functional assessment plays a crucial role in
52 the identification of cardiac toxicity and, more importantly, in the prediction of early cardiac
53 injury following chemotherapy[2]. However, current approaches for cardiac functional assessment
54 encounter limitations. Methods such as left ventricular ejection fraction (LVEF) provide only
55 global and often delayed cardiac mechanics after injury[3,4]. Tissue Doppler imaging provides
56 segmental myocardial deformation information but suffers from significant intraobserver and
57 interobserver variability, in part due to ultrasound beam angle dependency[5]. Two-dimensional
58 (2D) speckle tracking utilizes the B-mode of echocardiography, which theoretically eliminates the
59 angle dependency, but its accuracy is limited by out-of-plane motion[6]. Therefore, a rigorous
60 approach for quantifying segmental cardiac function is lacking in both research and clinical
61 settings.
62
63 In this context, we developed a 4D quantification method for the analysis of segmental cardiac
64 function that we named displacement analysis of myocardial mechanical deformation
65 (DIAMOND), to determine the displacement vectors of myocardial mass centroids in 3D space.
66 We applied DIAMOND for the in vivo assessment of cardiac function and doxorubicin-induced
67 cardiac toxicity with zebrafish (*Danio rerio*) as the animal model, chosen due to their regenerating
68 myocardium and highly conserved developmental genes[7]. We further compared segmental
69 DIAMOND displacement with global ejection fraction (EF) determination and 2D strain following
70 doxorubicin treatment. By integrating DIAMOND displacement with 4D light-sheet fluorescent
71 microscopy (LSFM) acquired rendering of embryonic zebrafish hearts, DIAMOND shows that the
72 basal myocardial segments adjacent to the atrioventricular canal undergo the highest mechanical
73 deformation and are the most susceptible to acute doxorubicin cardiac injury[8].
74
75 **PROTOCOL:**
76
77 All methods described here have been approved by the UCLA Institutional Animal Care and Use
78 Committee (IACUC), and experiments were performed in compliance with protocols approved by
79 the UCLA Office of Animal Research.
80
81 **1. Breeding *Tg(cmlc2:mCherry)* zebrafish and collection of embryos**
82
83 1.1. Follow the housing, breeding, and embryo collection procedures as described in previously
84 established husbandry and breeding practices. For details, see Messerschmidt et al.[9].
85
86 1.2. Treat the collected embryos with 0.003% 1-phenyl-2-thiourea (PTU) in E3 medium 18 h
87 postfertilization to maintain the transparency of the embryos for LSFM imaging.
88

89   **2. Doxorubicin treatment to induce cardiac injury**

91   2.1. At 3 days postfertilization (dpf), treat the embryos with doxorubicin at a concentration of 10
92   µM in E3 fish water medium. After a 24 h treatment to 4 dpf, replace the doxorubicin medium
93   with fresh E3 medium.

95   CAUTION: Doxorubicin is a chemotherapy medication. Appropriate personal protective
96   equipment (PPE) is required and the waste should be disposed of in biohazard waste containers.

98   **3. Notch pathway modulation**

100 3.1. Treat zebrafish embryos with the Notch pathway inhibitor (2S)-N-[(3,5-
101 difluorophenyl)acetyl]-L-alanyl-2-phenyl]glycine 1,1-dimethylethyl ester (DAPT) at a
102 concentration of 10 µM in E3 fish water medium from 3–6 dpf.

104 3.2. Microinject the Notch downstream effectors *Notch intracellular domain (NICD)* and
105 *Neuregulin-1 (Nrg-1)* mRNA at concentrations of 10 pg/nL and 5 pg/nL, respectively, into the 1-
106 cell stage zebrafish embryos[8,10].

108 NOTE: The microinjection is performed under a microscope with the support of an air pump to
109 accurately control the volume injected. The mRNA microinjection into the cell is done when the
110 fertilized egg is at the first cell stage. For details on the preparation and sequence of the mRNAs,
111 see Chen et al.[8]. For details on the microinjection and preparation of injection needles, see Rosen
112 et al.[10].

114 **4. LSFM imaging and post-imaging synchronization**

116 4.1. For the LSFM imaging techniques and post-imaging synchronization algorithm, see details in
117 previous publications[9,11].

119 NOTE: Briefly, our system utilizes a continuous-wave laser as the illumination source to image all
120 transgenic zebrafish lines. The detection module is composed of two scientific complementary
121 metal-oxide semiconductor (sCMOS) cameras and two sets of filters for dual-channel imaging.
122 The detection module is perpendicularly installed to the illumination plane. Each LSFM frame is
123 acquired within a 20 msec exposure time, while the resolving power in cross section is ~0.65 µm
124 and the step size between consecutive frames is ~2 µm. A 589 nm laser was used to excite
125 mCherry fluorescent signals.

127 **5. Reconstruction of the 3D systolic and diastolic heart**

129 5.1. Open the folder created by the post synchronization algorithm, then open the **"Output"**
130 folder. Select the middle plane of the heart and load the entire folder into ImageJ. Find the first
131 diastolic and systolic phase and record the frame number.

133	5.2. Open the "Output/By State" folder and find the folders that have the same numbers as the
134	frame numbers just recorded. Convert the images in the folder into 3D TIFF (tagged image file
135	format) files and name them "diastole.tif" and "systole.tif".
136	
137	**6. Segmentation of the ventricle**
138	
139	6.1. Open the image analyzing software (see **Table of Materials**). Click **File	Open data**, and load
140	"diastole.tif" and "systole.tif". Enter the voxel size according to the imaging settings.
141	
142	NOTE: For the LSFM system used, the typical voxel size is 0.65 µm x 0.65 µm x 2 µm.
143	
144	6.2. Click the "**SEGMENTATION**" panel and manually segment out the ventricle part of the heart.
145	The built-in "**Threshold**" tool that can select all the regions above a certain intensity can facilitate
146	this process. The ventricle is the thicker chamber with a stronger fluorescence.
147	
148	NOTE: Make sure to remove the atrioventricular canal and the outflow tract in the segmented
149	ventricle, because this affects the displacement analysis.
150	
151	6.3. After the segmentation is done, click the "**Project**" panel. Right click the "**diastole.Labels.tif**"
152	and "**systole.Labels.tif**" tabs in the console and click "**Export Data as**" to save the data as 3D TIFF
153	files.
154	
155	**7. Creation of rectangular parallelepipeds for image registration**
156	
157	7.1. Run "**prepImage_1.m**" in the programming environment (see **Table of Materials**). Open
158	"**prepImage_1.m**", "*ImPath*" in line 5 so the folder contains the original and segmented TIFF files,
159	and change *"slice"* in line 4 to the number of slices of the 3D tif files.
160	
161	7.2. After running the code, it will generate five new 3D TIFF files ("test.tif", "diastole_200.tif",
162	"systole_200.tif", "diaLabel.tif", and "sysLabel200.tif") as well as two new folders
163	("resample_dia" and "resample_sys").
164	
165	**8. Resample systolic and diastolic 3D hearts along the short axis plane**
166	
167	8.1. Import all five 3D TIFF files into the image analyzing software (see **Table of Materials**).
168	
169	NOTE: The voxel size is unchanged.
170	
171	8.2. Go to the **MULTIPLANAR** panel. Choose "diastole_200.tif" as the primary data. Align the X-
172	axis (the green line in the XY plane) with the vertical long axis of the ventricle, and align the Z-
173	axis (the red line in the YZ plane) with the horizontal long axis of the ventricle.
174	
175	NOTE: The vertical long axis is determined by finding the longest axis connecting the apex and
176	the outflow tract in the XY plane, and the horizontal long axis is determined by finding the longest

177 axis connecting the apex and the outflow tract in the YZ plane. Rotate the axis by placing the
178 cursor at the end of the axis.

179

180 8.3. Choose three random points from the oblique YZ plane (the short axis plane) in a
181 counterclockwise manner and record their 3D position coordinates.

182

183 NOTE: Make sure the points are chosen in a counterclockwise manner.

184

185 8.4. Repeat steps 8.2 and 8.3 for "systole_200.tif".

186

187 8.5. Click the "**PROJECT**" panel. Create a "**Slice**" object for "diastole_200.tif" by right clicking on
188 "diastole_200.tif" and searching for "**Slice**" object. Left click the Slice object just created, and in
189 the **Properties panel | Options**, check "**Set Plane**" and choose three points in "**Plane Definition**".
190 Enter the coordinates of the three points from step 7.3.

191

192 8.6. Repeat step 8.5 for "systole_200.tif".

193

194 NOTE: The slice object created should have the name "**Slice 2**".

195

196 8.7. Right click "diastole_200.tif" and search for "**Resample Transformed Image**" and create the
197 object. In the **Properties** panel, choose "**Slice**" as the "**Reference**" and click **Apply**. This should
198 generate an object named "**diastole_200.transformed**".

199

200 8.8. Right click "**diastole_200.transformed**" and search for "**Resample**" and create the object.
201 Choose "**Voxel Size**" as the "**Mode**" and change "**Voxel Size**" to be x = 1, y = 1, and z = 1 in the
202 **Properties** panel.

203

204 8.9. Click "**Apply**". This should generate an object named "**diastole_200.resampled**". Right click
205 "diastole_200.resampled" and save it as a 3D TIFF file.

206

207 8.10. Repeat the same step for "diaLabel.tif" and "test.tif". Save "diaLabel.resampled" and
208 "test.resampled" as 3D TIFF files. Repeat the same step for "systole_200.tif", "sysLabel.tif", and
209 "test.tif" using "**Slice 2**" as a reference, and save "systole_200.resampled", "sysLable.resampled",
210 and "test2.resampled" as 3D TIFF files.

211

212 NOTE: Make sure there are a total of six TIFF files saved in this step.

213

214 **9. Division of the resampled heart**

215

216 9.1. Import all six resampled files from step 8 to ImageJ. Select a slice of "systole_200.resampled"
217 in which the atrioventricular canal is clearly visualized. Record the number of the slice.

218

219 9.1.1. Use the "**Image|Transform|Rotate**" function of ImageJ so that the atrioventricular canal
220 is vertical. Apply the same rotation to all files. Close all windows and save all changes.

221

222 9.1.2. Move "diastole_200.resampled", "diaLabel.resampled", and "test.resampled" to the
223 "resample_dia" folder, and move "systole_200.resampled", "sysLable.resampled", and
224 "test2.resampled" to the "resample_sys" folder.

225

226 9.2. Open "divider_2_8_pieces.m". Change "**ImPath**" in line 5 and "**ImPath**" in line 395 to the
227 image directory. Change the variable "**Middle**" in line 22 and line 411 to the slice numbers where
228 the atrioventricular canal is clearly visualized in "systole_200.resampled" and
229 "diastole_200.resampled".

230

231 9.3. Run the code, and in the prompted windows click once at the center of the ventricle and
232 click once at the center of the atrioventricular canal. This needs to be done twice for both systole
233 and diastole images.

234

235 **10. Registration of systolic and diastolic image matrices**

236

237 10.1. Open "register_3.m" and change "**ImPath**" in line 4 to the image folder path. It might take
238 5–20 min to run this code depending on the computation power of the system.

239

240 NOTE: The artificially created rectangular parallelepipeds in step 7 are used for 3D rigid
241 registration that preserves the distance between two points and angles subscribed by three
242 points. When the end-diastole rectangular parallelepiped (red) is registered to the end-systole
243 rectangular parallelepiped (green), the ensuing discrepant 3D location permits the derivation of
244 a unique matrix of rigid transformation consisting of rotation and translation from the end-
245 diastole matrix to the end-systole matrix (**Figure 1H**). We perform the registration and
246 regularized energy minimization to denoise the matrix after the transformation using an image
247 processing toolbox (see **Table of Materials**). For a detailed mathematical description, please see
248 Chen et al.[8].

249

250 **11. Output of the displacement vectors**

251

252 11.1. Open "**displacement_4.m**" and change "**ImPath**" in line 4 to the image folder path.

253

254 11.2. Run "**displacement_4.m**", which generates a "vector8.txt" file in the "vectors" folder. Once
255 the "vector8.txt" file is open, there will be an 8 x 4 matrix. Each row of the matrix has four
256 numbers, which are the magnitudes of the X component, Y component, Z component, and the
257 SUM magnitude of the displacement vector of a specific segment of the ventricle.

258

259 NOTE: The displacement vector is obtained by calculating the displacement of the mass centroid
260 of each segment in 3D space. We calculate the 3D mass centroid (P_S and P_D) coordinates $\overline{P}_k$
261 (where k indicates the X, Y, or Z coordinate, respectively) of each segment (I-VI) in the
262 segmentation dataset from systole to diastole (**Figure 1J**). We define the mass centroid $\overline{P}_k$ in 3D
263 space as follows:

264

$$\overline{C_k} = \frac{1}{M_i} \sum_{j=1}^{m} C_{kj} \rho\left(x_j, y_j, z_j\right)$$

where $C_x = X$, $C_y = Y$, and $C_z = Z$, M_i = the mass of each segment ($I \leq i \leq VI$), m = the number of voxels of each segment, and ρ = the density function as the segmented region is 1 whereas the rest is 0. The L2-norm of the sub-displacement vectors along the X-, Y-, and Z-axes and the sum displacement vector are calculated during the cardiac cycle. There are a total of eight rows in the matrix. The first row and the eighth row contain the atrioventricular canal and are thus ignored in our analysis. Segments I to VI are represented by the second row to the seventh row.

REPRESENTATIVE RESULTS:

The process by which DIAMOND was developed to assess 3D segmental cardiac function is presented in **Figure 1**. Following LSFM image acquisition and reconstruction in 3D of the embryonic zebrafish heart (**Figure 1A**), the true short axis plane was determined as the plane perpendicular to the vertical and horizontal long axes, both of which are determined in a multiplane viewer (**Figure 1B**). The heart was then resampled along the short axis plane (**Figure 1C**), and divided into eight equal segments constituted by even angles according to a virtual division line (red dotted line) connecting the center of the endocardial ventricular cavity to the center of the atrioventricular canal (**Figure 1E**). The 3D depictions of the identified segments are illustrated in a cross-sectional view (**Figure 1F**) and in comparison with the raw data (**Figure 2**). Segments VII and VIII were removed from the analysis because they encompass the atrioventricular canal and thus contain less myocardium compared with other segments. The different resampling planes for end-systole (H_S) and end-diastole (H_D) lead to distinct coordinate systems for end-systolic and end-diastolic matrixes, which need to be registered to restore their original spatial relationship (**Figure 1G**). The coordinate system of the end-systolic matrix was chosen as the reference for consistency. To determine the transformation matrix (T_m) from the end-diastolic matrix to the end-systolic matrix, a matrix of three parallelepipeds, which is asymmetrical in 3D and has the same dimension as the original image matrix, was virtually created. The parallelepipeds were resampled twice, first in the short axis plane of the end-systole matrix, and then in the short axis plane of the end-diastole matrix, leading to different transformed parallelepipeds for end-systole (green) and end-diastole (red) (**Figure 1H**).

The green and red parallelepipeds were then registered together by a rigid body registration algorithm and T_m was calculated and applied to the end-diastole matrix to restore the coordinates (**Figure 1I**). This process permits subsequent tracking in the 3D space of the displacement vectors of mass centroids from any segment of the ventricle during the cardiac cycle (**Figure 1J**). DIAMOND displacement of ventricular segments I–VI can be tracked during multiple time points in the cardiac cycle (**Figure 1K**), which can be simplified for quantitative analysis to two time points ranging from end-systole to end-diastole (**Figure 1L**). The segments generated by DIAMOND can be visualized in **Figure 2**, where each color represent one cardiac segment.

With DIAMOND, we uncovered segmental heterogeneity of cardiac function and susceptibility to

307 doxorubicin-induced myocardial injury in zebrafish. Following a 24 h treatment with 10 μM
308 doxorubicin from 3–4 dpf (**Figure 3A**), we compared DIAMOND displacement of ventricular
309 segments between control and chemotherapy-treated groups (**Figure 3B**) and 48 h after
310 treatment (**Figure 3C**). All DIAMOND figures follow the same graphical pattern as the resampled
311 ventricles along the short axis (**Figure 1E**). The data are presented as percentages by normalizing
312 the L2-norm of the displacement vector to the inner perimeter of the heart, with the X (green),
313 Y (blue), and Z components (orange) illustrated as their weighted contributions. At 4 dpf, the
314 average L2-norm of the segmental displacement vectors in control fish ranged from 6.6–11.3 μm,
315 or 3.8–6.6% after normalization. Our results indicate that under control conditions, the basal
316 segments I and VI undergo the largest displacements and are the ones most susceptible to
317 doxorubicin induced cardiac injury (**Figure 3B**, 29% decrease from 6.6–4.7%, n = 10 control and n
318 = 8 doxorubicin, $p < 0.01$). At 6 dpf, the average L2-norm of the segmental displacement vectors
319 in the control fish ranged from 6.8–14 μm, or 3.9–8% after normalization. At 6 dpf, the basal
320 segments I and VI recovered DIAMOND displacement to control levels, suggesting segmental
321 regeneration (**Figure 3C**, n = 10 control and n = 8 doxorubicin). In parallel, a worsening in 2D basal
322 strain from -53 to -38% was observed at 4 dpf following doxorubicin treatment, followed by a
323 return to control levels at 6 dpf, corroborating the DIAMOND displacement results (**Figure 3D**,
324 **3E**). A parallel decrease in global ejection fraction in response to doxorubicin at 4 dpf with
325 recovery at 6 dpf was also observed (**Figure 3F**, **3G**).

327 We next applied DIAMOND during doxorubicin treatment and Notch pathway modulation using
328 the Notch inhibitor DAPT and rescue using Notch downstream effectors *NICD* and *NRG1* mRNA
329 (**Figure 4A**). *NICD* and *NRG1* mRNA microinjection rescued the decrease in DIAMOND
330 displacement and EF after acute chemotherapy-induced injury at 4 dpf (**Figure 4B**, **4D**). Exposure
331 to the Notch inhibitor DAPT together with doxorubicin led to a more diffuse decrease in
332 DIAMOND displacement, in addition to the basal segments I and VI (**Figure 4B**). Moreover,
333 inhibition of the Notch pathway after chemo-induced injury further hindered the recovery of
334 DIAMOND displacement of the basal segments and EF at 6 dpf. The inhibition was rescued by the
335 Notch downstream effectors *NICD* and *NRG1* (**Figure 4C**, **4E**).

337 **FIGURE AND TABLE LEGENDS:**
338 **Figure 1: 4D DIAMOND displacement development.** (**A**) Raw images were captured by light-
339 sheet fluorescent microscopy. (**B** and **C**) Reconstructed 3D heart was resampled along the true
340 short axis plane view. (**D**) Schematic illustration of embryonic zebrafish heart. (**E** and **F**) 2D and
341 3D illustrations of the division of the ventricle into eight segments excluding segments VII and
342 VIII. (**G**) The different coordinate systems of end-systole and end-diastole after resampling. (**H**) A
343 group of rectangular parallelepipeds was created for the generation of a transformation matrix
344 (T_m). (**I**) Registered end-systolic and end-diastolic coordinate systems by applying T_m. (**J**)
345 Displacement vector of the segmental mass centroid from end-systole to end-diastole. (**K**)
346 DIAMOND displacement of ventricular segments I–VI tracked during multiple time points in the
347 cardiac cycle. (**L**) DIAMOND displacement of ventricular segments I–VI from end-systole to end-
348 diastole. This figure from Chen et al.[8] is reproduced with permission from the American Society
349 for Clinical Investigation (ASCI).

351   **Figure 2: DIAMOND segmentation of the embryonic zebrafish heart compared with raw data**
352   **in 3D.** The embryonic zebrafish heart was divided into six segments (volumes) depicted here in
353   different colors for the calculation of DIAMOND displacements (left). The displacement vector of
354   each segment computed by DIAMOND represents its segmental cardiac function. The atrium and
355   outflow tract were removed during segmentation. Scale bar = 50 μm.

356

357   **Figure 3: DIAMOND unravels the segmental heterogeneity in cardiac function and susceptibility**
358   **to chemotherapy-induced injury.** (**A**) Experimental schedule of doxorubicin treatment. (**B** and **C**)
359   Segmental comparison of DIAMOND displacement vectors normalized to the inner myocardial
360   perimeter between control and doxorubicin-treated groups at 4 and 6 dpf (t tests, **$p < 0.01$, n
361   = 8–10 per group). (**D** and **E**) Assessment of strain in the ventricular base depicting a similar injury
362   and regeneration pattern as the DIAMOND displacement vectors (*$p < 0.05$, n = 6–8 per group).
363   (**F** and **G**) Decrease in ejection fraction in response to doxorubicin at 4 dpf with recovery at 6 dpf,
364   following a pattern similar to segmental DIAMOND displacements at the global ventricular level
365   (t tests, **$p < 0.01$, error bars SEM, n = 6–10 per group). This figure from Chen et al.[8] is
366   reproduced with permission from the ASCI.

367

368   **Figure 4: DIAMOND mechanics for assessment of Notch-mediated myocardial recovery**
369   **following doxorubicin-induced injury.** (**A**) Experimental schedule. (**B** and **C**) *NICD* and *NRG1*
370   Notch downstream effectors rescued the reduction of DIAMOND displacement in segments I and
371   VI at 4 dpf. At 6 dpf, inhibition of Notch signaling by DAPT impaired the restoration of segmental
372   cardiac function (ANOVA, **$p < 0.01$ Dox vs. control; †$p < 0.05$, ††$p < 0.01$, Dox + DAPT vs. control,
373   n = 6–10 per group). (**D** and **E**) Ejection fraction corroborates DIAMOND mechanics at the global
374   level (ANOVA, *$p < 0.05$, **$p < 0.01$, error bars SEM, n = 5–11 per group). This figure from Chen
375   et al.[8] is reproduced with permission from the ASCI.

376

377   **DISCUSSION:**
378   A rigorous strategy for quantification of segmental myocardial function is critical to assess cardiac
379   mechanics beyond traditional EF, known to be an insensitive and delayed indicator of myocardial
380   injury[1,4,12]. Hence, there has been a growing interest in markers of early myocardial changes, and
381   a growing body of literature supports myocardial deformation parameters as an early indicator
382   to forecast ventricular dysfunction[4,13]. Echocardiographic measurement of left ventricular (LV)
383   strain provides an established method of myocardial deformation measurement[13]. However,
384   tissue Doppler-based strain imaging suffers from a number of shortcomings due to angle
385   dependency and intraobserver and interobserver variability[14]. Speckle tracking
386   echocardiography (STE) can resolve angle-independent 2D and 3D tissue deformation, but the
387   accuracy of 2D speckle tracking is affected by through-plane motion[6], while 3D speckle tracking
388   requires superior spatial resolution to resolve the positive ultrasound interference patterns
389   (speckles) in 3D and high temporal resolution to track the speckles between frames[15]. In the
390   present protocol, we describe DIAMOND displacement as a novel myocardial deformation
391   parameter for in vivo quantification of 4D segmental cardiac function in zebrafish. Compared
392   with EF and 2D strain as reference standards, DIAMOND provides additional segmental
393   deformation information without being affected by through-plane motion. By integrating
394   DIAMOND with 4D LSFM, our technique can assess the displacement vector of a heart segment

395   20–30 μm in width, which is currently impossible for even the most advanced 3D STE system,
396   which has millimeter-range resolution[16].
397
398   To apply DIAMOND, it is critical to have a comprehensive understanding of the anatomical
399   structure of the embryonic zebrafish heart. During image segmentation, it is essential that the
400   atrioventricular canal and the outflow tract are correctly identified and segmented out from the
401   rest of the myocardium when the user is performing step 6 in the protocol. Furthermore, the
402   horizontal and the vertical long axes of the ventricle must be accurately determined in order to
403   derive the true short axis plane for image resampling in step 8.
404
405   The major rate limiting factor of applying DIAMOND is the manual segmentation of the ventricle,
406   which becomes time-consuming when multiple phases during the cardiac cycle may need to be
407   evaluated. With the advancement of machine learning and neural networks, an automated
408   cardiac segmentation method[17,18,19,20] could be integrated with DIAMOND to provide monitoring
409   of segmental cardiac function throughout the entire cardiac cycle. Further applications of
410   DIAMOND also include the integration with echocardiography, micro-CT, or micro-MRI, suitable
411   in larger animal models for the multiscale assessment of cardiac injury and regeneration[21].
412   However, the method will first require adaptation to the presence of myocardial fibers leading
413   to more complex cardiac deformation including torsion in mammals[22,23].
414
415   Overall, DIAMOND provides a novel method to evaluate segmental cardiac function in embryonic
416   zebrafish under both physiological and pathological conditions and may be used as a platform for
417   high-throughput in vivo screening of pathways associated with chemotherapy-induced cardiac
418   toxicity.
419

424
425   **DISCLOSURES:**
426   The authors have declared that no conflict of interest exists.
427

428   **REFERENCES:**
429   Ewer, M. S., Ewer, S. M. Cardiotoxicity of anticancer treatments. *Nature Reviews Cardiology.* **12**
430   (9), 547–558 (2015).
431   Thavendiranathan, P., Wintersperger Bernd, J., Flamm Scott, D., Marwick Thomas, H. Cardiac MRI
432   in the Assessment of Cardiac Injury and Toxicity From Cancer Chemotherapy. *Circulation:*
433   *Cardiovascular Imaging.* **6** (6), 1080–1091 (2013).
434   Mickoleit, M. et al. High-resolution reconstruction of the beating zebrafish heart. *Nature*
435   *Methods.* **11** (9), 919–922 (2014).
436   Thavendiranathan, P. et al. Use of Myocardial Strain Imaging by Echocardiography for the Early
437   Detection of Cardiotoxicity in Patients During and After Cancer Chemotherapy. *A Systematic*
438   *Review.* **63** (25 Part A), 2751–2768 (2014).

439 Collier, P., Phelan, D., Klein, A. A Test in Context: Myocardial Strain Measured by Speckle-Tracking
440 Echocardiography. *Journal of the American College of Cardiology.* **69** (8), 1043–1056 (2017).
441 Hanekom, L., Cho, G. Y., Leano, R., Jeffriess, L., Marwick, T. H. Comparison of two-dimensional
442 speckle and tissue Doppler strain measurement during dobutamine stress echocardiography: an
443 angiographic correlation. *European Heart Journal.* **28** (14), 1765–1772 (2007).
444 Poss, K. D., Wilson, L. G., Keating, M. T. Heart regeneration in zebrafish. *Science.* **298** (5601),
445 2188–2190 (2002).
446 Chen, J. et al. Displacement analysis of myocardial mechanical deformation (DIAMOND) reveals
447 segmental susceptibility to doxorubicin-induced injury and regeneration. *JCI Insight.* **4** (8), (2019).
448 Messerschmidt, V. et al.Light-sheet Fluorescence Microscopy to Capture 4-Dimensional Images
449 of the Effects of Modulating Shear Stress on the Developing Zebrafish Heart. *Journal of Visualized*
450 *Experiments.* (138), e57763 (2018).
451 Rosen, J. N., Sweeney, M. F., Mably, J. D. Microinjection of Zebrafish Embryos to Analyze Gene
452 Function. *Journal of Visualized Experiments.* (25), e1115 (2009).
453 Lee, J. et al. 4-Dimensional light-sheet microscopy to elucidate shear stress modulation of cardiac
454 trabeculation. *The Journal of Clinical Investigation.* **126** (5), 1679–1690 (2016).
455 Lenneman, C. G., Sawyer, D. B. Cardio-Oncology: An Update on Cardiotoxicity of Cancer-Related
456 Treatment. *Circulation Research*. **118** (6), 1008–1020 (2016).
457 Geyer, H. et al. Assessment of Myocardial Mechanics Using Speckle Tracking Echocardiography:
458 Fundamentals and Clinical Applications. *Journal of the American Society of Echocardiography.* **23**
459 (4), 351–369 (2010).
460 Castro, P. L., Greenberg, N. L., Drinko, J., Garcia, M. J., Thomas, J. D. Potential pitfalls of strain
461 rate imaging: angle dependency. *Biomedical Sciences Instrumentation.* **36**, 197–202 (2000).
462 Seo, Y., Ishizu, T., Aonuma, K. Current Status of 3Dimensional Speckle Tracking Echocardiography:
463 A Review from Our Experiences. *Journal of Cardiovascular Ultrasound.* **22** (2), 49–57 (2014).
464 Amzulescu, M. S. et al. Improvements of Myocardial Deformation Assessment by Three-
465 Dimensional Speckle-Tracking versus Two-Dimensional Speckle-Tracking Revealed by Cardiac
466 Magnetic Resonance Tagging. *Journal of the American Society of Echocardiography.* **31** (9), 1021–
467 1033.e1021 (2018).
468 Wolterink, J. M., Leiner, T., Viergever, M. A., Išgum, I. in *Reconstruction, Segmentation, and*
469 *Analysis of Medical Images.* Eds. Maria A. Zuluaga et al.) 95–102 (Springer International
470 Publishing).
471 Avendi, M. R., Kheradvar, A., Jafarkhani, H. A combined deep-learning and deformable-model
472 approach to fully automatic segmentation of the left ventricle in cardiac MRI. *Medical Image*
473 *Analysis.* **30**, 108–119 (2016).
474 Packard, R. R. S. et al. Automated Segmentation of Light-Sheet Fluorescent Imaging to
475 Characterize Experimental Doxorubicin-Induced Cardiac Injury and Repair. *Scientific Reports*. **7**
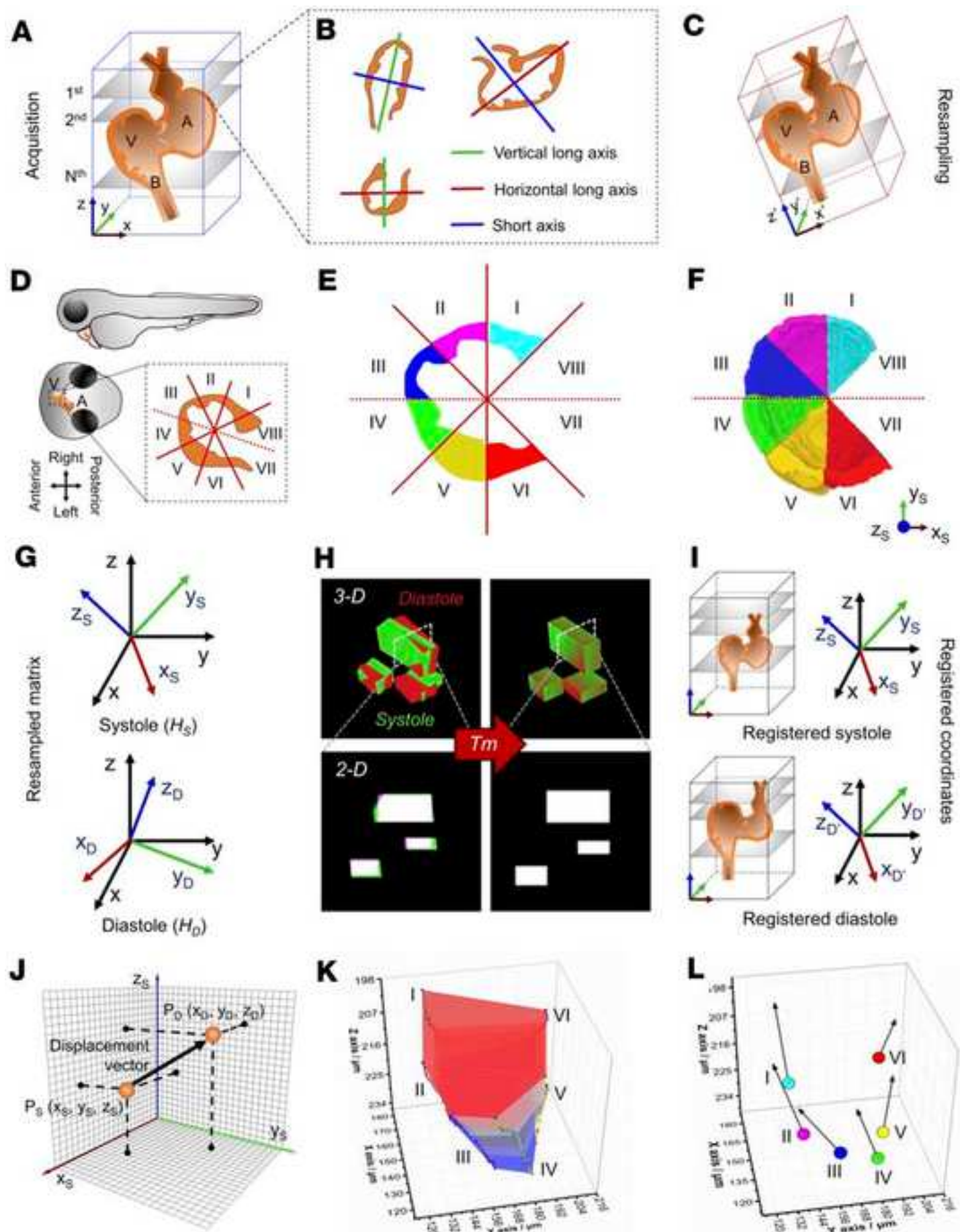476 (1), 8603 (2017).
477 Jay Kuo, C. C., Chen, Y. On data-driven Saak transform. *Journal of Visual Communication and*
478 *Image Representation*. **50**, 237–246 (2018).
479 Natarajan, N. et al. Complement Receptor C5aR1 Plays an Evolutionarily Conserved Role in
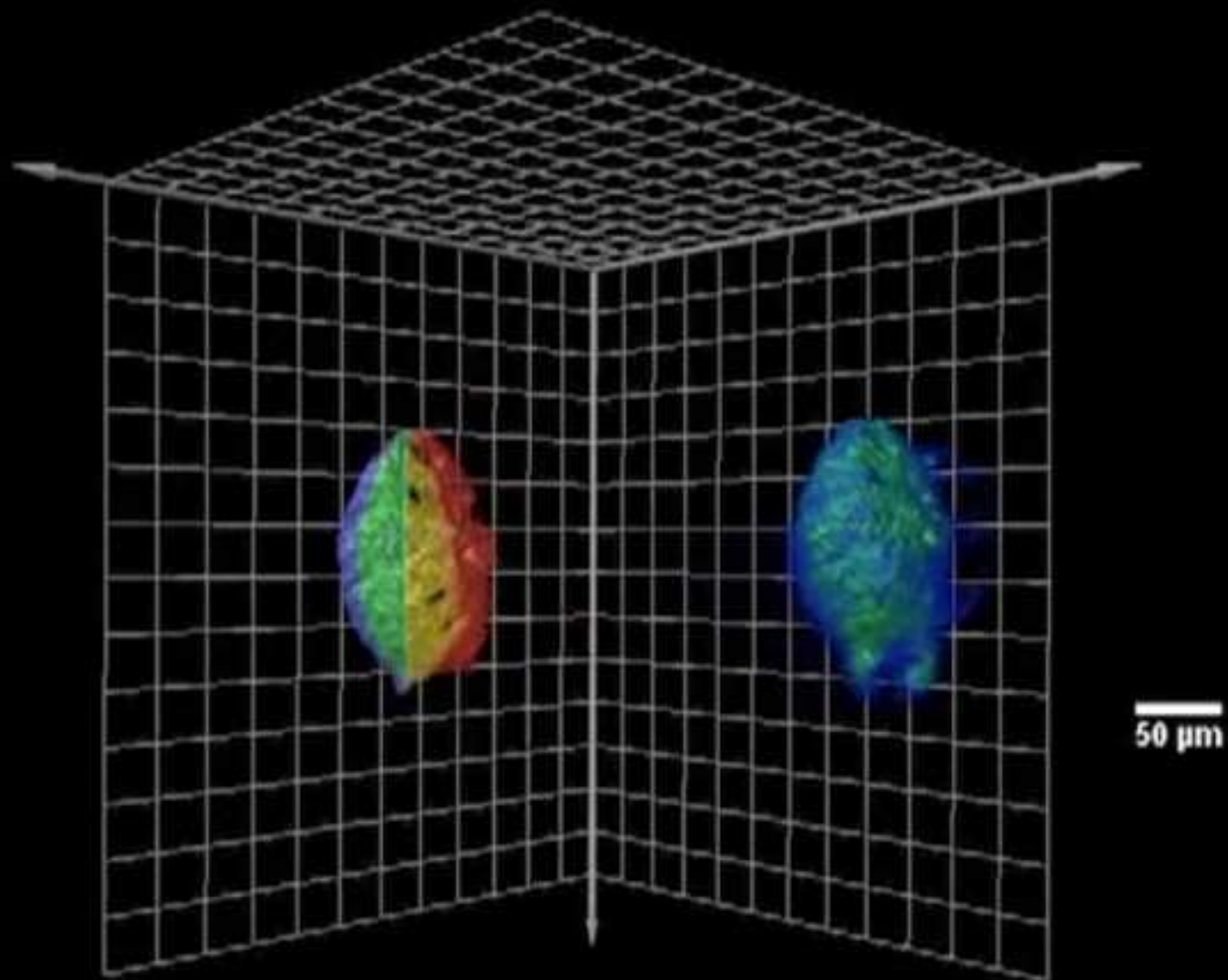480 Successful Cardiac Regeneration. *Circulation.* **137** (20), 2152–2165 (2018).
481 Zhukov, L., Barr, A. H. in *IEEE Visualization*. VIS 2003. 597–602 (2003).
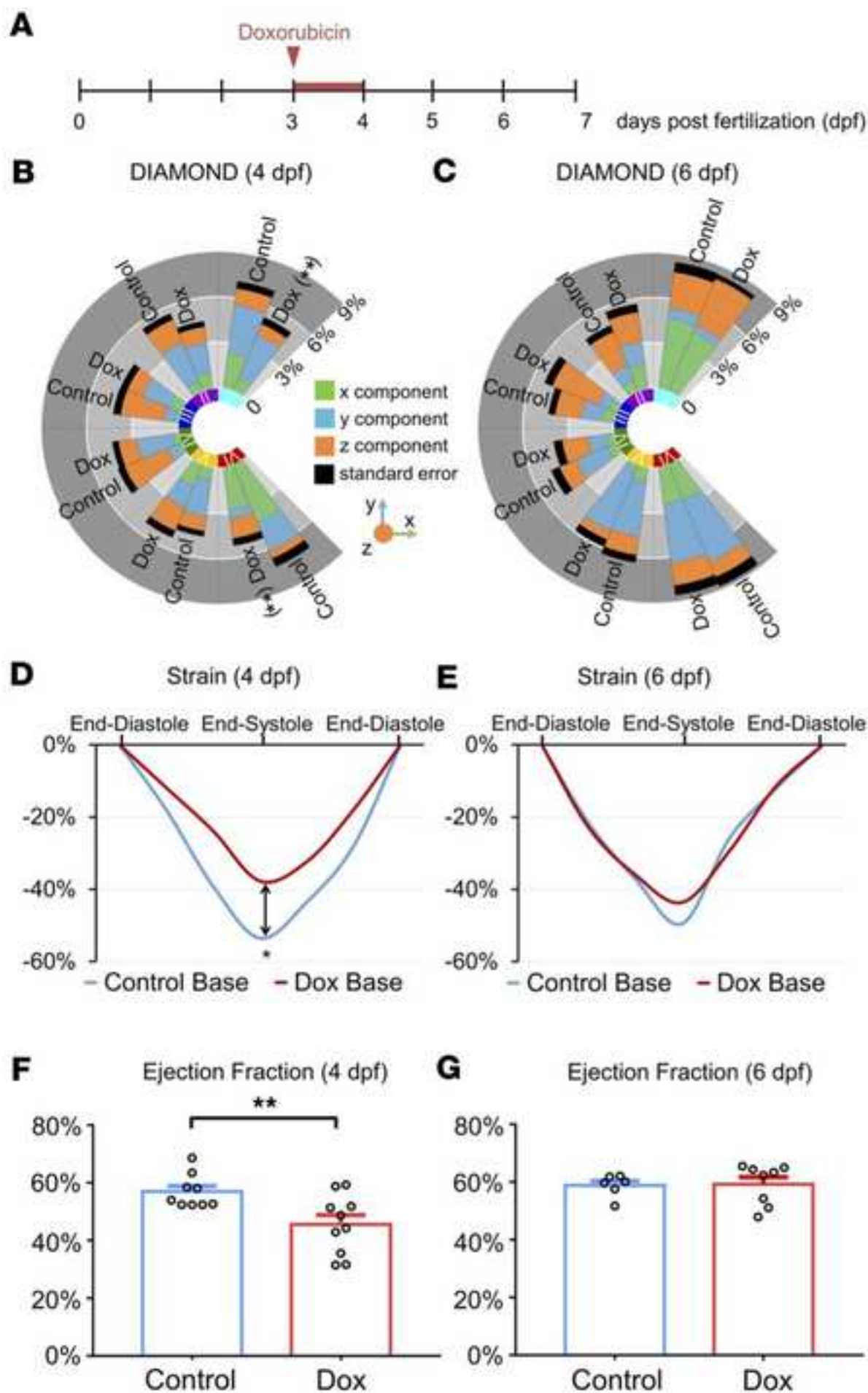482 23   Nielles-Vallespin, S. et al. In vivo diffusion tensor MRI of the human heart: Reproducibility

483   of breath-hold and navigator-based approaches. *Magnetic Resonance in Medicine*. **70** (2), 454–
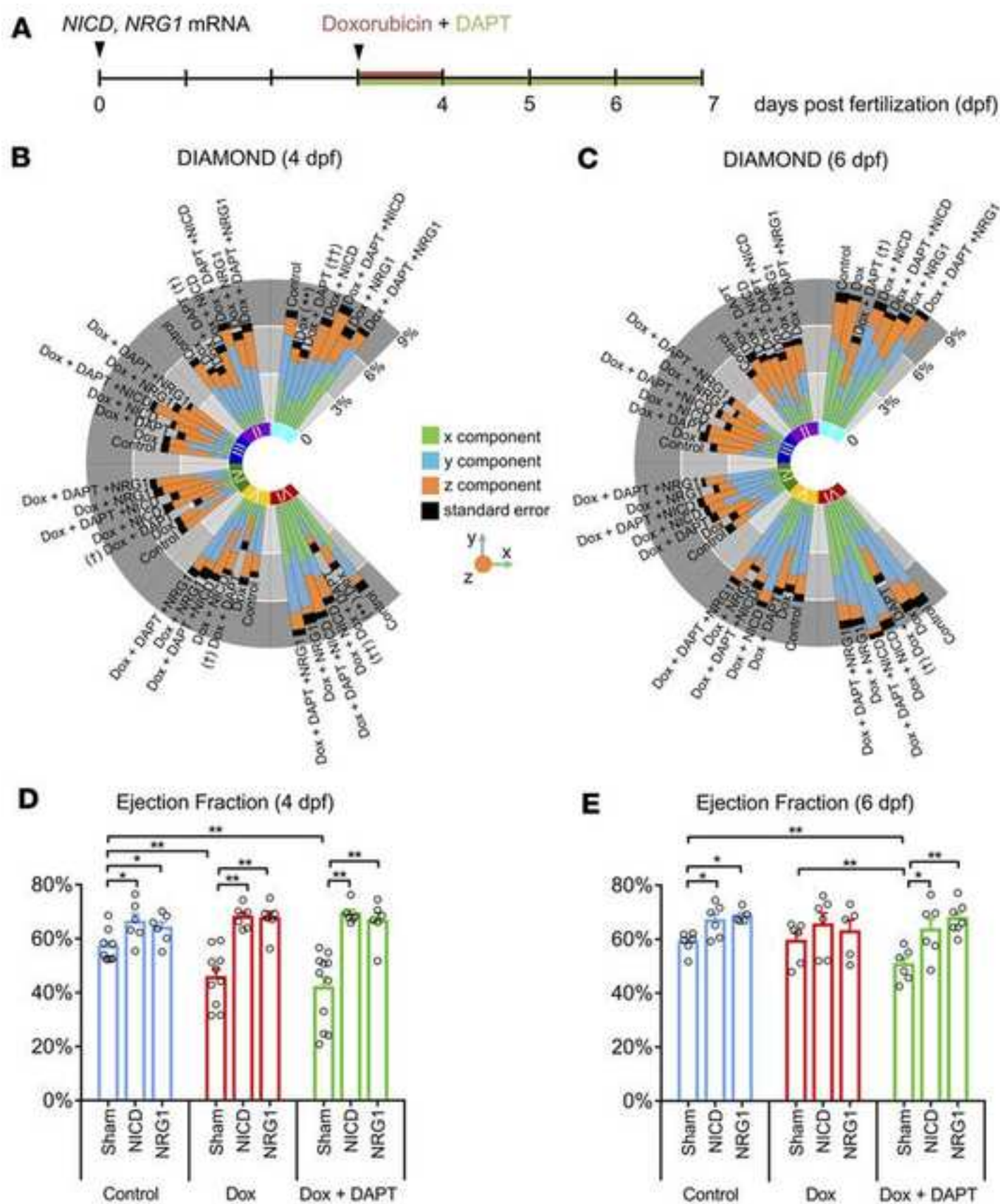484   465 (2013).

A NICD, NRG1 mRNA   Doxorubicin + DAPT

days post fertilization (dpf)

B DIAMOND (4 dpf)

C DIAMOND (6 dpf)

- x component
- y component
- z component
- standard error

D Ejection Fraction (4 dpf)

Sham NICD NRG1 | Sham NICD NRG1 | Sham NICD NRG1
Control | Dox | Dox + DAPT

E Ejection Fraction (6 dpf)

Sham NICD NRG1 | Sham NICD NRG1 | Sham NICD NRG1
Control | Dox | Dox + DAPT

Name of Material/Equipment	Company	Catalog Number	Comments/Description
Amira6	FEI		Image analyzing software
DAPT	Millipore Sigma	D5942-5MG	
Doxorubicin hydrochloride	Millipore Sigma	D1515-10MG	
Ethyl 3-aminobenzoate methanesulfonate	Millipore Sigma	E10521-10G	Tricaine
MATLAB	MathWorks		Programming environment
MATLAB Image Processing Toolbox	MathWorks		Image processing toolbox

jove
VISUALIZED EXPERIMENTS

1 Alewife Center #200
Cambridge, MA 02140
tel 617.945.9051
www.jove.com

ARTICLE AND VIDEO LICENSE AGREEMENT

Title of Article: DISPLACEMENT ANALYSIS OF MYOCARDIAL MECHANICAL DEFORMATION (DIAMOND) REVEALS SEGMENTAL HETEROGENEITY OF CARDIAC FUNCTION IN EMBRYONIC ZEBRAFISH

Author(s): JUNJIE CHEN, RENE R. SEVAG PACKARD

Item 1: The Author elects to have the Materials be made available (as described at http://www.jove.com/publish) via:

[X] Standard Access   [ ] Open Access

Item 2: Please select one of the following items:

[ ] The Author is **NOT** a United States government employee.

[ ] The Author is a United States government employee and the Materials were prepared in the course of his or her duties as a United States government employee.

[X] The Author is a United States government employee but the Materials were NOT prepared in the course of his or her duties as a United States government employee.

ARTICLE AND VIDEO LICENSE AGREEMENT

1.   **Defined Terms.** As used in this Article and Video License Agreement, the following terms shall have the following meanings: "**Agreement**" means this Article and Video License Agreement; "**Article**" means the article specified on the last page of this Agreement, including any associated materials such as texts, figures, tables, artwork, abstracts, or summaries contained therein; "**Author**" means the author who is a signatory to this Agreement; "**Collective Work**" means a work, such as a periodical issue, anthology or encyclopedia, in which the Materials in their entirety in unmodified form, along with a number of other contributions, constituting separate and independent works in themselves, are assembled into a collective whole; "**CRC License**" means the Creative Commons Attribution-Non Commercial-No Derivs 3.0 Unported Agreement, the terms and conditions of which can be found at: http://creativecommons.org/licenses/by-nc-nd/3.0/legalcode; "**Derivative Work**" means a work based upon the Materials or upon the Materials and other pre-existing works, such as a translation, musical arrangement, dramatization, fictionalization, motion picture version, sound recording, art reproduction, abridgment, condensation, or any other form in which the Materials may be recast, transformed, or adapted; "**Institution**" means the institution, listed on the last page of this Agreement, by which the Author was employed at the time of the creation of the Materials; "**JoVE**" means MyJove Corporation, a Massachusetts corporation and the publisher of The Journal of Visualized Experiments; "**Materials**" means the Article and / or the Video; "**Parties**" means the Author and JoVE; "**Video**" means any video(s) made by the Author, alone or in conjunction with any other parties, or by JoVE or its affiliates or agents, individually or in collaboration with the Author or any other parties, incorporating all or any portion of the Article, and in which the Author may or may not appear.

2.   **Background.** The Author, who is the author of the Article, in order to ensure the dissemination and protection of the Article, desires to have the JoVE publish the Article and create and transmit videos based on the Article. In furtherance of such goals, the Parties desire to memorialize in this Agreement the respective rights of each Party in and to the Article and the Video.

3.   **Grant of Rights in Article.** In consideration of JoVE agreeing to publish the Article, the Author hereby grants to JoVE, subject to **Sections 4** and **7** below, the exclusive, royalty-free, perpetual (for the full term of copyright in the Article, including any extensions thereto) license (a) to publish, reproduce, distribute, display and store the Article in all forms, formats and media whether now known or hereafter developed (including without limitation in print, digital and electronic form) throughout the world, (b) to translate the Article into other languages, create adaptations, summaries or extracts of the Article or other Derivative Works (including, without limitation, the Video) or Collective Works based on all or any portion of the Article and exercise all of the rights set forth in (a) above in such translations, adaptations, summaries, extracts, Derivative Works or Collective Works and(c) to license others to do any or all of the above. The foregoing rights may be exercised in all media and formats, whether now known or hereafter devised, and include the right to make such modifications as are technically necessary to exercise the rights in other media and formats. If the "Open Access" box has been checked in **Item 1** above, JoVE and the Author hereby grant to the public all such rights in the Article as provided in, but subject to all limitations and requirements set forth in, the CRC License.

4. **Retention of Rights in Article.** Notwithstanding the exclusive license granted to JoVE in **Section 3** above, the Author shall, with respect to the Article, retain the non-exclusive right to use all or part of the Article for the non-commercial purpose of giving lectures, presentations or teaching classes, and to post a copy of the Article on the Institution's website or the Author's personal website, in each case provided that a link to the Article on the JoVE website is provided and notice of JoVE's copyright in the Article is included. All non-copyright intellectual property rights in and to the Article, such as patent rights, shall remain with the Author.

5. **Grant of Rights in Video – Standard Access.** This **Section 5** applies if the "Standard Access" box has been checked in **Item 1** above or if no box has been checked in **Item 1** above. In consideration of JoVE agreeing to produce, display or otherwise assist with the Video, the Author hereby acknowledges and agrees that, Subject to **Section 7** below, JoVE is and shall be the sole and exclusive owner of all rights of any nature, including, without limitation, all copyrights, in and to the Video. To the extent that, by law, the Author is deemed, now or at any time in the future, to have any rights of any nature in or to the Video, the Author hereby disclaims all such rights and transfers all such rights to JoVE.

6. **Grant of Rights in Video – Open Access.** This **Section 6** applies only if the "Open Access" box has been checked in **Item 1** above. In consideration of JoVE agreeing to produce, display or otherwise assist with the Video, the Author hereby grants to JoVE, subject to **Section 7** below, the exclusive, royalty-free, perpetual (for the full term of copyright in the Article, including any extensions thereto) license (a) to publish, reproduce, distribute, display and store the Video in all forms, formats and media whether now known or hereafter developed (including without limitation in print, digital and electronic form) throughout the world, (b) to translate the Video into other languages, create adaptations, summaries or extracts of the Video or other Derivative Works or Collective Works based on all or any portion of the Video and exercise all of the rights set forth in (a) above in such translations, adaptations, summaries, extracts, Derivative Works or Collective Works and (c) to license others to do any or all of the above. The foregoing rights may be exercised in all media and formats, whether now known or hereafter devised, and include the right to make such modifications as are technically necessary to exercise the rights in other media and formats. For any Video to which this **Section 6** is applicable, JoVE and the Author hereby grant to the public all such rights in the Video as provided in, but subject to all limitations and requirements set forth in, the CRC License.

7. **Government Employees.** If the Author is a United States government employee and the Article was prepared in the course of his or her duties as a United States government employee, as indicated in **Item 2** above, and any of the licenses or grants granted by the Author hereunder exceed the scope of the 17 U.S.C. 403, then the rights granted hereunder shall be limited to the maximum rights permitted under such statute. In such case, all provisions contained herein that are not in conflict with such statute shall remain in full force and effect, and all provisions contained herein that do so conflict shall be deemed to be amended so as to provide to JoVE the maximum rights permissible within such statute.

8. **Protection of the Work.** The Author(s) authorize JoVE to take steps in the Author(s) name and on their behalf if JoVE believes some third party could be infringing or might infringe the copyright of either the Author's Article and/or Video.

9. **Likeness, Privacy, Personality.** The Author hereby grants JoVE the right to use the Author's name, voice, likeness, picture, photograph, image, biography and performance in any way, commercial or otherwise, in connection with the Materials and the sale, promotion and distribution thereof. The Author hereby waives any and all rights he or she may have, relating to his or her appearance in the Video or otherwise relating to the Materials, under all applicable privacy, likeness, personality or similar laws.

10. **Author Warranties.** The Author represents and warrants that the Article is original, that it has not been published, that the copyright interest is owned by the Author (or, if more than one author is listed at the beginning of this Agreement, by such authors collectively) and has not been assigned, licensed, or otherwise transferred to any other party. The Author represents and warrants that the author(s) listed at the top of this Agreement are the only authors of the Materials. If more than one author is listed at the top of this Agreement and if any such author has not entered into a separate Article and Video License Agreement with JoVE relating to the Materials, the Author represents and warrants that the Author has been authorized by each of the other such authors to execute this Agreement on his or her behalf and to bind him or her with respect to the terms of this Agreement as if each of them had been a party hereto as an Author. The Author warrants that the use, reproduction, distribution, public or private performance or display, and/or modification of all or any portion of the Materials does not and will not violate, infringe and/or misappropriate the patent, trademark, intellectual property or other rights of any third party. The Author represents and warrants that it has and will continue to comply with all government, institutional and other regulations, including, without limitation all institutional, laboratory, hospital, ethical, human and animal treatment, privacy, and all other rules, regulations, laws, procedures or guidelines, applicable to the Materials, and that all research involving human and animal subjects has been approved by the Author's relevant institutional review board.

11. **JoVE Discretion.** If the Author requests the assistance of JoVE in producing the Video in the Author's facility, the Author shall ensure that the presence of JoVE employees, agents or independent contractors is in accordance with the relevant regulations of the Author's institution. If more than one author is listed at the beginning of this Agreement, JoVE may, in its sole

jove

1 Alewife Center #200
Cambridge, MA 02140
tel 617 945 9051
www.jove.com
VISUALIZED EXPERIMENTS

ARTICLE AND VIDEO LICENSE AGREEMENT

discretion, elect not take any action with respect to the Article until such time as it has received complete, executed Article and Video License Agreements from each such author. JoVE reserves the right, in its absolute and sole discretion and without giving any reason therefore, to accept or decline any work submitted to JoVE. JoVE and its employees, agents and independent contractors shall have full, unfettered access to the facilities of the Author or of the Author's institution as necessary to make the Video, whether actually published or not. JoVE has sole discretion as to the method of making and publishing the Materials, including, without limitation, to all decisions regarding editing, lighting, filming, timing of publication, if any, length, quality, content and the like.

12.   **Indemnification.** The Author agrees to indemnify JoVE and/or its successors and assigns from and against any and all claims, costs, and expenses, including attorney's fees, arising out of any breach of any warranty or other representations contained herein. The Author further agrees to indemnify and hold harmless JoVE from and against any and all claims, costs, and expenses, including attorney's fees, resulting from the breach by the Author of any representation or warranty contained herein or from allegations or instances of violation of intellectual property rights, damage to the Author's or the Author's institution's facilities, fraud, libel, defamation, research, equipment, experiments, property damage, personal injury, violations of institutional, laboratory, hospital, ethical, human and animal treatment, privacy or other rules, regulations, laws, procedures or guidelines, liabilities and other losses or damages related in any way to the submission of work to JoVE, making of videos by JoVE, or publication in JoVE or elsewhere by JoVE. The Author shall be responsible for, and shall hold JoVE harmless from, damages caused by lack of sterilization, lack of cleanliness or by contamination due to

the making of a video by JoVE its employees, agents or independent contractors. All sterilization, cleanliness or decontamination procedures shall be solely the responsibility of the Author and shall be undertaken at the Author's expense. All indemnifications provided herein shall include JoVE's attorney's fees and costs related to said losses or damages. Such indemnification and holding harmless shall include such losses or damages incurred by, or in connection with, acts or omissions of JoVE, its employees, agents or independent contractors.

13.   **Fees.** To cover the cost incurred for publication, JoVE must receive payment before production and publication of the Materials. Payment is due in 21 days of invoice. Should the Materials not be published due to an editorial or production decision, these funds will be returned to the Author. Withdrawal by the Author of any submitted Materials after final peer review approval will result in a US$1,200 fee to cover pre-production expenses incurred by JoVE. If payment is not received by the completion of filming, production and publication of the Materials will be suspended until payment is received.

14.   **Transfer, Governing Law.** This Agreement may be assigned by JoVE and shall inure to the benefits of any of JoVE's successors and assignees. This Agreement shall be governed and construed by the internal laws of the Commonwealth of Massachusetts without giving effect to any conflict of law provision thereunder. This Agreement may be executed in counterparts, each of which shall be deemed an original, but all of which together shall be deemed to me one and the same agreement. A signed copy of this Agreement delivered by facsimile, e-mail or other means of electronic transmission shall be deemed to have the same legal effect as delivery of an original signed copy of this Agreement.

A signed copy of this document must be sent with all new submissions. Only one Agreement is required per submission.

CORRESPONDING AUTHOR

Name:	RENE R. SEVAG PACKARD, MD, PhD
Department:	MEDICINE - CARDIOLOGY
Institution:	UNIVERSITY OF CALIFORNIA, LOS ANGELES
Title:	ASSISTANT PROFESSOR-IN-RESIDENCE
Signature:	*[signature]*	Date:	7. 9. 2019
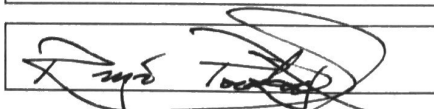
Please submit a **signed** and **dated** copy of this license by one of the following three methods:
1. Upload an electronic version on the JoVE submission site
2. Fax the document to +1.866.381.2236
3. Mail the document to JoVE / Attn: JoVE Editorial / 1 Alewife Center #200 / Cambridge, MA 02140

We thank the Editor and the Reviewers for their time and expert comments. We have addressed all the points raised in a systematic manner.

Editor's comments:

Comment 1
Protocol Language: Please re-write ALL text in the protocol in the imperative voice/tense as if you are telling someone how to do the technique (i.e. "Do this", "Measure that" etc.) Any text that cannot be written in the imperative tense may be added as a "Note", however, notes should be used sparingly and actions should be described in the imperative tense wherever possible.
1) For example: 1.2: Treat the collected embryos with 0.003% 1-phenyl-2-thiourea (PTU, Sigma-Aldrich) in E3 medium 18 hours post fertilization to maintain the transparency of the embryos for LSFM imaging.

Response 1
We have fixed the imperative voice/tense in the manuscript based on the editor's comments.

Comment 2
Protocol Detail: Please note that your protocol will be used to generate the script for the video, and must contain everything that you would like shown in the video. Please add more specific details (e.g. button clicks for software actions, numerical values for settings, etc) to your protocol steps. There should be enough detail in each step to supplement the actions seen in the video so that viewers can easily replicate the protocol. Some examples:
1) 3.1: define DAPT.
2) 3.2: How exactly was microinjection performed? Was this done under a microscope? Was the injection manual or was a syringe pump used? Where in the body do you inject? Mention needle gauge. Are the zebra fish anesthetized? If so, how?
3) Section 4: Given the goals laid out in the summary " to detail a novel method for the assessment of segmental cardiac function in embryonic zebrafish under both physiological and pathological conditions"; the protocol is incomplete without a more detailed description of the LSFM imaging technique. This can be brief, however, the current description is insufficient.

Response 2
1) DAPT is a γ-secretase inhibitor, and its full name is (2S)-N-[(3,5-Difluorophenyl)acetyl]-L-alanyl-2-phenyl]glycine 1,1-dimethylethyl ester. We have defined its full name in the manuscript.
2) We have added the following text into the manuscript Protocol Section 3.2:
'The microinjection is performed under a microscope with the support of an air pump to accurately control the volume injected. The microinjection is done when the fertilized egg is at the first cell stage, at which time the mRNA is injected into the cell. […] For details on the microinjection and preparation of injection needles, see Rosen *et al*.'
3) We have added a more detailed description of the LSFM imaging technique in Protocol Section 4.1:
'Briefly, our system utilizes a continuous-wave laser as the illumination source to image all transgenic zebrafish lines. The detection module is composed of two scientific complementary metal-oxide semiconductor (sMOS) cameras and two sets of filters for dual-channel imaging. The detection module is perpendicularly installed to the illumination plane. Each LSFM frame is acquired within a 20 msec exposure time, while the resolving power in cross-section is ~ 0.65 μm and the step size between consecutive frames is ~2 μm.'

Reference
Rosen, J. N., *et al*. Microinjection of Zebrafish Embryos to Analyze Gene Function. *JoVE*. doi:10.3791/1115 (25), e1115, (2009).

Comment 3
Protocol Highlight: After you have made all of the recommended changes to your protocol (listed above), please re-evaluate the length of your protocol section. There is a 10-page limit for the protocol text, and a 3- page limit for filmable content. If your protocol is longer than 3 pages, please highlight ~2.5 pages or less of text (which includes headings and spaces) in yellow, to identify which steps should be visualized to tell the most cohesive story of your protocol steps.
1) The highlighting must include all relevant details that are required to perform the step. For example, if step 2.5 is highlighted for filming and the details of how to perform the step are given in steps 2.5.1 and 2.5.2, then the sub-steps where the details are provided must be included in the highlighting.
2) The highlighted steps should form a cohesive narrative, that is, there must be a logical flow from one highlighted step to the next.
3) Please highlight complete sentences (not parts of sentences). Include sub-headings and spaces when calculating the final highlighted length.
4) Notes cannot be filmed and should be excluded from highlighting.
5) Please bear in mind that software steps without a graphical user interface/calculations/ command line scripting cannot be filmed.
6) Please edit the title to focus on the highlighted portions of the protocol.

Response 3
We have re-evaluated the length of the protocol section and made sure that it dose not exceed the page limit. We have revised the protocol based on the editor's suggestions.

Comment 4
Discussion: JoVE articles are focused on the methods and the protocol, thus the discussion should be similarly focused. Please ensure that the discussion covers the following in detail and in paragraph form (3-6 paragraphs): 1) modifications and troubleshooting, 2) limitations of the technique, 3) significance with respect to existing methods, 4) future applications and 5) critical steps within the protocol.

Response 4
We have revised the discussion based on the editor's suggestions.

Comment 5
Figures: define all error bars.

Response 5
All error bars have been defined in the figure legends.

Comment 6
Commercial Language: JoVE is unable to publish manuscripts containing commercial sounding language, including trademark or registered trademark symbols (TM/R) and the mention of company brand names before an instrument or reagent. Examples of commercial sounding language in your manuscript are Sigma-Aldrich, Amira (FEI), MATLAB, 1) Please use MS Word's find function (Ctrl+F), to locate and replace all commercial sounding language in your manuscript with generic names that are not company-specific. All commercial products should be sufficiently referenced in the table of materials/reagents. You may use the generic term followed by "(see table of materials)" to draw the readers' attention to specific commercial names.

Response 6
We have removed all commercial sounding languages and the products have been referred to in the Table of Materials.

Comment 7
Table of Materials: Please revise the table of the essential supplies, reagents, and equipment. The table should include the name, company, and catalog number of all relevant materials/software in separate columns in an xls/xlsx file. Please include items such as software, instruments, zebrafish rearing reagents, etc

Response 7
The Table of Materials has been revised based on the editor's comments.

Comment 8
Please define all abbreviations at first use.

Response 8
All abbreviations have been properly defined at first use.

Reviewers' comments:

Reviewer #1:

General Comments
The manuscript describes a procedure to analyze mechanical deformation from images of zebrafish hearts. As such, this is an important endeavor, and a useful tool for people analyzing the biomechanics of heart development, especially those using zebrafish - although it is likely adaptable to other species and images (future work). However, the manuscript falls short in explaining even in general terms the assumptions behind the algorithms employed: a better description of intended registration and simplifications is required. As it stands the paper is merely a manual for a very specific software and a VERY specific example - if someone wants to deviate from this example, it is not clear he/she will have the tools to properly use the software as no guidance is provided.

Response
We thank the reviewer for the supportive comments. To address the reviewer's concerns regarding the details of the algorithms, we have revised and added multiple sections of the manuscript (Protocol sections 8.3, 8.6, 10.1, 11.2). These provide the reader with further details and explanations regarding the algorithms, and thus more freedom to deviate from them as appropriate for a different set of experiments.

Major Comments

The paper does not really describe the main idea behind the program/algorithm. The paper should state the main principles use to calculate/estimate deformation. Instead, the paper goes into excruciating details of how to upload the data into the program, how to rotate the heart, etc. It never describes how the registration is performed, and how corresponding points/regions are determined by the algorithm. This is probably mathematically complex, and does not need to be specified in detail, but at least give an idea of how these steps are done internally. This will be valuable for the user as well, who will be able to focus on important issues for instance during the initial manual alignment, which is probably crucial for the analysis.

Response

We thank the reviewer for the opportunity for clarification. We have added the following description into the manuscript Protocol Section step 10.1:

'The artificially created rectangular parallelepipeds in step 7 are used for 3-D rigid registration which preserves the distance between two points and angles subscribed by three points. When the end-diastole rectangular parallelepiped (red) is registered to the end-systole rectangular parallelepiped (green), the ensuing discrepant 3-D location permits the derivation of a unique matrix of rigid transformation consisting of rotation and translation from the end-diastole matrix to the end-systole matrix (Figure 1H). We performed the registration and regularized energy minimization (to denoise the matrix after the transformation) using the image processing toolbox (see Table of Materials). For a detailed mathematical description of the above process, please see Chen *et al*.'

Reference

Chen, J. *et al.* Displacement analysis of myocardial mechanical deformation (DIAMOND) reveals segmental susceptibility to doxorubicin-induced injury and regeneration. *JCI Insight*. **4** (8), (2019).

Minor Comment 1

What do you mean by 'focal cardiac mechanics'? I do not think the algorithm is doing that - but perhaps adding an explanation will help clarify.

Response 1

We thank the reviewer for the opportunity for clarification. To this end, we have removed 'focal' and 'local' from the manuscript and use only 'segmental'.
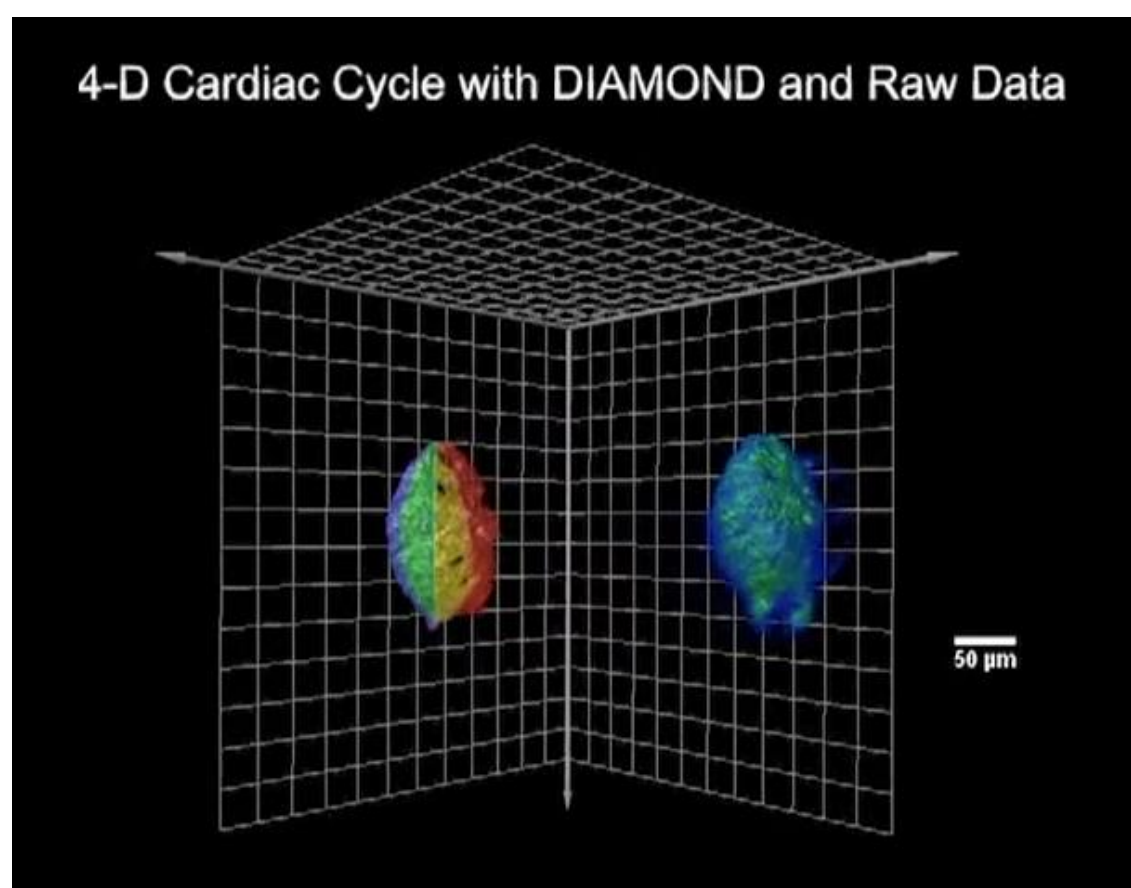
Minor Comment 2

What is 'segmental cardiac function'?

Response 2

We thank the reviewer for the opportunity to further expand this concept. Given Figure 2 provides the best visualization to address this question, we have revised the Figure 2 legend for further clarification:

'The embryonic zebrafish heart was divided into six segments (volumes) depicted here with different colors for the calculation of DIAMOND displacements (left). The displacement vector of each segment computed by DIAMOND represents its segmental cardiac function.'

We also present Figure 2 below for visual depiction.

Minor Comment 3
Sections 4 to 11. I understand that the algorithms are described in previous publications, however, a very brief description of them is necessary here. This is kind of a user manual, that does not give you any clue of what you are doing or why. The steps specify opening of folders and the such, it would be beneficial to know what the folders contain exactly, for example, "image stacks containing a 3D reconstruction of the heart at diastole". Not in excruciating detail, but briefly.

Response 3
We appreciate the reviewer's comment. We have added the following description of the algorithm into Protocol Section step 10.1:
'The artificially created rectangular parallelepipeds in step 7 are used for 3-D rigid registration which preserves the distance between two points and angles subscribed by three points. When the end-diastole rectangular parallelepiped (red) is registered to the end-systole rectangular parallelepiped (green), the ensuing discrepant 3-D location permits the derivation of a unique matrix of rigid transformation consisting of rotation and translation from the end-diastole matrix to the end-systole matrix (Figure 1H). We perform the registration and regularized energy minimization (to denoise the matrix after the transformation) using the image processing toolbox (see Table of Materials). For a detailed mathematical description, please see Chen *et al.*'
This description is also used to address reviewer 1's major comment.
We also added the following description to Protocol section 11.2:
'The displacement vector is obtained by calculating the displacement of the mass centroid of each segment in 3D space. We calculate the 3-D mass centroid (P_S and P_D) coordinates $\overline{C_k}$ (where k indicates the x, y, or z coordinate, respectively) of each segment (I-VI) in the segmentation dataset from systole to diastole (Figure 1J). We define the mass centroid $\overline{C_k}$ in 3-D space as follows:

$$\overline{C_k} = \frac{1}{M_i}\sum_{j=1}^{m} C_{kj}\rho(x_j, y_j, z_j)$$

where $C_x = x$, $C_y = y$, and $C_z = z$, M_i is the mass of each segment (I ≤ i ≤ VI), m is interpreted as the number of voxels of each segment, and ρ denotes the density function as the segmented region is 1 whereas the rest is 0. The L2-norm of the sub-displacement vectors along the x-, y-, z-axis and the sum displacement vector are calculated during the cardiac cycle.'

Reference
Chen, J. *et al.* Displacement analysis of myocardial mechanical deformation (DIAMOND) reveals segmental susceptibility to doxorubicin-induced injury and regeneration. *JCI Insight.* **4** (8), (2019).

Minor Comments 4 and 5
Section 8. This step is likely critical. The reader should be reminded of important issues to take into account. "Make sure to...." Also, what exactly needs to be accomplished here? Some guidance will be beneficial.
Same as above for Sections 9 to 11.

Responses 4 and 5
We thank the reviewer for this valuable comment. This step is to correctly find the true short axis planes for both systolic and diastolic hearts and to resample the hearts along the short axis planes. We have added several important notes for this step into the manuscript as follows:
• In step 8.3: 'Make sure the points are chosen in a counterclockwise manner'.
• In step 8.8: 'Make sure there are total 6 TIFF files saved in this step'.

Minor Comment 6
Results. I do not understand what are the 'segments' and what they represent. Are they volumetric regions? How exactly are they defined?

Response 6
This description is also used to address reviewer 1's minor comment 2. Given Figure 2 provides the best visualization to address this question, we have revised the Figure 2 legend for further clarification:
'The embryonic zebrafish heart was divided into six segments (volumes) depicted here with different colors for the calculation of DIAMOND displacements (left). The displacement vector of each segment computed by DIAMOND represents its segmental cardiac function.'

Minor Comment 7
How is the registration performed? How are the mass centroids determined and why?

Response 7
The below description is also used to address reviewer 1's minor comment 3. We have added the following description into the manuscript step 11.2:

'The displacement vector is obtained by calculating the displacement of the mass centroid of each segment in 3D space. We calculated the 3-D mass centroid (P_S and P_D) coordinates $\overline{C_k}$ (where k indicates the x, y, or z coordinate, respectively) of each segment (I-VI) in the segmentation dataset from systole to diastole (Figure 1J). We define the mass centroid $\overline{C_k}$ in 3-D space as follows:

$$\overline{C_k} = \frac{1}{M_i} \sum_{j=1}^{m} C_{kj} \rho(x_j, y_j, z_j)$$

where $C_x = x$, $C_y = y$, and $C_z = z$, M_i is the mass of each segment (I ≤ i ≤ VI), m is interpreted as the number of voxels of each segment, and ρ denotes the density function as the segmented region is 1 whereas the rest is 0. The L2-norm of the sub-displacement vectors along the x-, y-, z-axis and the sum displacement vector are calculated during the cardiac cycle'.

Reviewer #2:

General Comments
DIAMOND is interesting method to uncover cardiac functions from optical technique. Authors have used light-sheet microscopy and zebrafish animal model to demonstrate the cardiac mechanics after treating Doxorubicine which is commonly used for chemotherapy. Using DIAMOND method, the authors have compared cardiac mechanics such as displacement vectors of segmented areas. It has been well-tested with sham model, Doxo-treated model, DAPT treated model, and rescued models. However, I do have some minor concerned before publication.

Response
We thank the Reviewer for the supportive comments.

Minor Concern 1
Authors mentioned they adjust threshold to make fluorescent signal strong from weak fluorescent signal. This process possibly includes noise around stronger fluorescent signal. I was wondering if this affects the accuracy of DIAMOND analysis?

Response 1
We thank the reviewer for this valuable comment. We did not use the 'Threshold' tool mentioned in Protocol Section 6.2 to make 'weak' fluorescent signals 'strong'. Based on our experience, the fluorescent signal from *Tg(cmlc2:mCherry)* is sufficiently strong to clearly visualize the heart. The 'Threshold' tool was used to select all the regions above a certain intensity threshold in order to facilitate manual segmentation. Noise is removed afterwards manually, thus it should not affect the accuracy of DIAMOND. We have added the following description of the 'Threshold' tool to Protocol section 6.2: 'The built-in "Threshold" tool that can select all the regions above a certain intensity can facilitate this process'.

Minor Concern 2
It is clear how they determines short axis plane. However, it is not clear how to determine vertical and horizontal long axis. It is important to clarify because short axis plane is perpendicular to two planes.

Response 2
We thank the reviewer for this valuable comment. We have added this description into the manuscript section 8.2"
'The vertical long axis is determined by finding the longest axis connecting the apex and the outflow tract in the XY plane, and the horizontal long axis is determined by finding the longest axis connecting the apex and the outflow tract in the YZ plane'.

Reviewer #3:

General Comments
The authors set out to create an automatic method to calculate displacement strain from light sheet fluorescence microscopy images. The method (DIAMOND) is easy to use and clearly spelled out in the abstract. The program also calculates conventional cardiac function parameters such as volumes and ejection fraction. DIAMOND is robust and takes 4D data as input.

Response
We thank the Reviewer for the supportive comments.

Major Comment 1
Are there any issues or dependence of DIAMOND on light-sheet fluorescence microscopy parameters such as power, laser angle, or emission wavelength? If so, please recommend some optimal settings so that others can reproduce the robustness of the method.

Response 1
We thank the reviewer for this valuable comment. There is no dependence on the power of the LSFM system, as long as the laser intensity is sufficient enough to excite the fluorescent signal. The angle of the laser is always perpendicular to the camera. Emission wavelength should be determined by the fluorescent protein expressed by the sample, and the proper filter should be chosen to eliminate the background noise generated by the source laser. However, there is dependence on the resolution and image quality of the microscope, because a good image quality is essential for image segmentation and anatomical structure visualization. We recommend the lateral resolution to be at least 1 μm. We have added the description of the angle and wavelength to Protocol section 4.1.

Major comment 2
How do you deal with non-cyclical motion (i.e. arrhythmia)? It seems that the authors use a model that depends on cyclical repetitive motion to reconstruct different cardiac phases in 3D. My concern is when users apply DIAMOND to either early embryonic stages with pulsatile motion or mutation cases with arrhythmic heart rate.

Response 2
We agree with the reviewer that there might be concerns when DIAMOND is applied to those studies. During early embryonic stages, it is difficult to acquire high quality images given the heart is blocked by the yolk sac. We have tried to image 1 and 2 dpf zebrafish hearts with LSFM, but the image quality was subpar.
Most post-imaging reconstruction algorithms are based on the assumption that the heart is undergoing a cyclical repetitive motion. Because our current post-imaging processing algorithm also relies on this assumption, DIAMOND cannot be applied to arrhythmic hearts. If the reader would want to study arrhythmia in zebrafish using optical methods, the best currently available options are Electrically Tunable Lens-SPIM (ETL-SPIM) or light field microscopy. However, the ETL-SPIM system is technically challenging (Mickoleit *et al.*) and light field microscopy currently suffers from low spatial resolution. This should be an area of future research.

Reference
Mickoleit, M. *et al.* High-resolution reconstruction of the beating zebrafish heart. *Nat Methods.* **11** 919,(2014).